Revista Ingeniería de Construcción. RIC
Vol 37 Nº3 2022 www.ricuc.cl
DOI: 10.7764/RIC.00038.21

ENGLISH VERSION

Performance of a UHPFRC overlay in the rehabilitation of a typical asphalt pavement structure

Comportamiento mecánico de una estructura de pavimento flexible rehabilitada con una sobrecapa de UHPFRC

A. Meléndez [1*] https://orcid.org/0000-0001-6714-9393
L. Peña*
H. Vacca* https://orcid.org/0000-0003-3159-6997
Y. Alvarado* https://orcid.org/0000-0002-1260-8211

[*] *Pontificia Universidad Javeriana, Bogotá, COLOMBIA*

Fecha de Recepción:21/02/2022
Fecha de Aceptación: 18/05/2022
Fecha de publicación: 02/12/2022
PAG 333-344

Abstract

This study determine the mechanical performance of a 40 mm thick overlay using UHPFRC (Ultra High-Performance Concrete) as the outer surface for restoring a flexible pavement structure. A 30 m long test section was built, divided into two 15 m sections. Section 1 was restored with a 60 mm overlay of Hot Mix Asphalt -HMA- and Section 2 was restored with a 40 mm overlay of UHPFRC without intermediate transverse joins. The two sections were instrumented with pressure cells in order to evaluate the vertical load in the inner fiber of each restoration layer. The mechanical properties of the materials were evaluated, the structural modeling was carried out with the falling weight deflectometer (FWD) and the Bisar 3.0 software. The structural modeling showed an 82% increase in the lifecycle for the section restored with UHPFRC. The functional evaluation of the rehabilitated structures was carried out considering parameters as: friction, percentage of cracking, rutting, international roughness index -IRI- and smoothness.

Keywords*: Percentage of cracking; rutting; international roughness index IRI; smoothness.*

Resumen

Este estudio determinó el desempeño mecánico de una sobre capa de 40 mm ± 10 mm de espesor construida con UHPFRC (Ultra High Performance Fiber Reinforced Concrete, por sus siglas en inglés) como capa de rodadura en la rehabilitación de un pavimento flexible. Se construyó un tramo de prueba de 30 m de longitud, dividido en dos secciones de 15 m. Sección 1 rehabilitada con una sobre capa de 60 mm de Mezcla Asfáltica semi-densa en Caliente (MSC). Sección 2 rehabilitada con una sobre capa de 40 mm de UHPFRC sin juntas transversales intermedias. Las secciones fueron instrumentadas con celdas de presión para evaluar la presión vertical en la fibra inferior de cada sección. Se evaluaron las propiedades mecánicas de los materiales, se realizó la modelación estructural con el deflectómetro de impacto (FWD, por sus siglas en ingles). La modelación estructural indicó un incremento del 82% de la vida útil para la sección rehabilitada con UHPFRC. Adicionalmente, la evaluación funcional de las estructuras rehabilitadas se realizó teniendo en cuenta parámetros de fricción, porcentaje de fisuración, ahuellamiento, índice de rugosidad internacional -IRI- y lisura.

Palabras claves: Parámetros de fricción; porcentaje de fisuración; ahuellamiento; índice de rugosidad internacional IRI; lisura.

1. *Introduction*

Pavement rehabilitation is defined as the work required in order to improve structural and/or functional capacity characteristics of a pavement (Ahmed et ál., 2020). Among the different rehabilitation techniques, Whitetopping (WT) has been found to be a traditional overlay alternative with hot asphaltic mixes (HMA). WT technique consists in the overlaying of a hydraulic concrete layer over an existing flexible pavement structure in order to improve its structural and functional capacity, prolonging its useful life. WT is understood as the overlaying of concrete with thicknesses of 100 to 175 mm (Mateos et ál., 2019). Thicknesses below 102 mm are known as Ultra-Thin Whitetopping (UTW) (Khazanovich and Tompkins, 2017). This rehabilitation technique has presented some flaws such as chipping of corners produced by the stress concentration, fissures related to underlying layers, and a weak connection between HMA and UTW (Hungria et ál., 2020). Additionally, the contraction of hydraulic concrete induces tensile stresses in the interface of both materials and generates cracking, which it weakens its load capacity and permeates the pavement structure (Hungria et ál., 2020). Furthermore, the reduced size of slabs implies greater amounts of shear and increases construction costs (Hungria et ál., 2020).

[1] *Corresponding author:*
Pontificia Universidad Javeriana, Bogotá, COLOMBIA
E-mail: andresf_melendez@javeriana.edu.co

DOI: 10.7764/RIC.00038.21

Throughout the last decades, research efforts have been made in regards to new cementing materials with the purpose of overcoming the restrictions of conventional concrete. As a result of some of these studies (Koutný et ál., 2018); (Xue, et ál., 2020), the development of Ultra High-Performance Concrete (UHPC), and Ultra High-Performance Fiber Reinforced Concrete (UHPFRC) have been incorporated (Shi et ál., 2015); (Green et ál., 2014); (Graybeal, 2006), positioning itself as an important trend in modern civil engineering. UHPFRC are materials comprised of a dense, homogeneous and self-leveling matrix which is the result of combining cementing materials, fine aggregates, water reducing additives, metallic or organic fibers and with a typical water/binder between 0.14 - 0.20 (Shi et ál., 2015); (Zhou et ál., 2018). The inclusion of fibers is necessary in order to promote flexion resistance and provide

ductility to the material (Larsen and Thorstensen, 2020). The mechanical and durability properties of UHPFRC make it an alternative for rehabilitating ultra-thin layer pavement structures. Additionally, it has the potential for being used as one of the more sustainable construction materials, given that it aligns with social trends that favor fast paced construction, given pre-manufactured construction components and their ease of installing, while it keeps the promise of a reduced weight and lasting aesthetic (Quist Batista et ál., 2019).

The main uses of UHPFRC have focused in structural and architectural elements. However, their use as a pavement structure component has been limited to specific repairs and over bridge panel layers (Zhou et ál., 2018). Despite that there has been research developed on the use of UHPFRC as repair overlayer for panels in vehicle bridges. To the date, relevant information regarding the use of ultra-thin layers with UHPFRC with thicknesses below or equal to 50 mm as wearing course in rehabilitated pavement structures is limited; and its use has neither been compared with traditional rehabilitation methods with asphaltic mix. Therefore, this research had the main purpose of analyzing a UHPFRC overlayer in the rehabilitation of a flexible pavement and compared with conventional asphaltic mix rehabilitation, identifying structural performance and service live of two test sections 15 m long, installed on a national service roadway in the road corridor between Bogotá (Fontibón) – Facatativá – Los Alpes (Cundinamarca, Colombia).

2. Methods and Materials

2.1 Methodology

This subchapter was divided in a preliminary planning phase and the construction of the test section, and a fieldwork phase with both (2) substages of development. The first substage corresponded to modelling of structures; the second, to function evaluation of the section rehabilitated with UHPFRC.

In the planning phase, technical data and input parameters were compiled for the selection materials, occupation and construction permits for the test section located in the national category roadway, Bogotá (Fontibón)– Facatativá – Los Alpes (Cundinamarca, Colombia). The section was projected with two rehabilitation alternatives for an existing flexible pavement structure with a total length of 30 m and width of 3.45 m. This section was divided in two sections, each of 15 m long; the first section was rehabilitated with an overlay semi-dense type asphaltic mixture MSC – with a thickness of 60 mm (2.36 in), the second section was rehabilitated with an ultra-thin layer 40 mm (1.57 in) thick of UHPFRC. The structure was open to traffic after ten days of casting the UHPFRC overlay. (Figure 1) depicts details regarding the resulting structures and the location of cells in each part of the section.

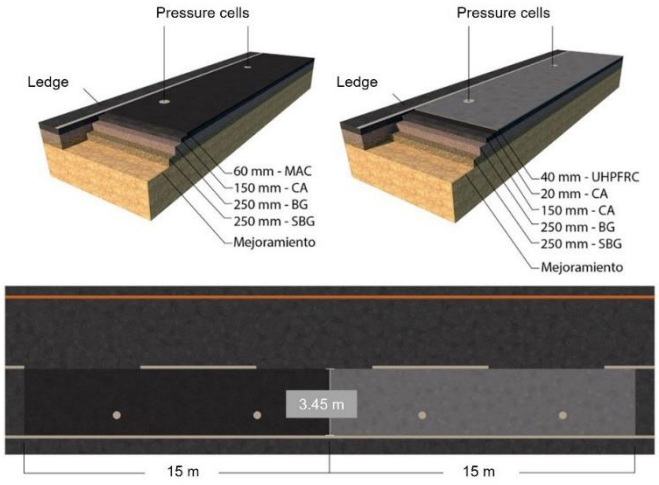

Figure 1. *Detail of rehabilitated sections and location of pressure cells*

DOI: 10.7764/RIC.00038.21

2.2 Modeling of resulting structures

Using the technique of back-calculation and Bisar 3.0 software, a residual life was established in terms of equivalent axis of 8.2 tons (80.4 kN) registering readings with FWD (Falling Weight Deflectometer) in each part of the section. As for the section rehabilitated with UHPFRC, several laboratory tests were performed for resistance to compression, flexion and the modulus of elasticity of field taken samples. For the use of MSC, a master curve of dynamic module and the characterization results of the installed mix (asphalt content, air voids percentage and unit weight) was adopted. The model was developed through a multilayer elastic analysis and was field verified with controlled load tests using a C3 type vehicle registering speed readings of 30, 60 and 80 km/h.

2.3 Functional evaluation of rehabilitated structures

The section rehabilitated with UHPFRC was spatially divided into 45 sections of 1.0 m x 1.15 m, each identified with a photographic registry code for evaluating surface changes during the study period. Follow up was conducted periodically each month during nine (9) months after opening the roadway for service, and a final checkup in 18 months of service.

Cracking parameters were evaluated by applying the PCI method, which establishes the condition of a pavement through a numeric index, based on a visual inventory that determines quantity, class and severity of damages present in pavement (Marcomini et al, 2020) and the International Roughness Index IRI, according to the ASTM E1926-08 (ASTM International, 2021) noem, through precision topographic leveling. Readings were taken every 250 mm throughout the 30 m of the test lane. In order to evaluate sliding resistance, a TRRL pendulum was used over MSC and three (3) readings were taken on its imprint in order to average the value. As for the UHPFRC, readings were taken at the start, middle and end of the section, placing the pendulum over the imprint and the central zone of the transversal lane section. Readings were taken each meter of the two sections for the smoothness study.

2.4 Materials and dosage

In conventional rehabilitation, a semi-dense hot asphaltic mix (MSC) was installed, with a maximum aggregate size of 19 mm and resilient modulus evaluated at 21°C and 10 Hz of 5,860 MPa (Table 1). Installed UHPFRC dosing is shown on (Table 2). The average compressive resistance of UHPFRC was 111 MPa, average flexural resistance pf 14 MPa and modulus of elasticity of 41,000 MPa (results at 28 days of aging). The characteristics of the metallic fiber are depicted on (Table 3).

Table 1. *Characteristics of the Hot Asphalt Mixture*

Mix Type	Asphalt Content (%)	Unit Weight (kg/m³)	Air voids percentage (%)
MSC	5.8	2,330	5.08

Table 2*. UHPFRC mix dosage*

Material	kg / m³
Water	211
Type III cement (ASTM C150)	711
Silica fume	232
Calcium carbonate	274
Fine aggregate	713
Superplasticizer agent *	20
Stell fiber	153

** Superplasticizer agent base don polycarboxylate manufactured for complying with ASTM C494 requirements for A type water reducer and F type high range water reducer*

Table 3. *Characterization of metallic fiber*

Dramix Fiber OL13/.2	
Fiber shape	Straight
Length (mm)	13
Diameter (mm)	0.20
Tensile stresses (N/mm2)	2750
Modulus of elasticity (GPa)	200

DOI: 10.7764/RIC.00038.21

2.4 *Equipment*

Milling was carried out with a Wirteng 150 milling MSChine and the MSC layer was installed with an asphalt finisher MSChine. MSC was compacted with a tandem vibro compactor of 8000 kg and a smooth pneumatic compactor of 10000 kg. UHPFRC was installed with an extender roller. No vibrating equipment was used. Measurement of deflections was carried out with a KUAM-50 impact deflectometer, which was setup for applying a 40 kN load.

Four (4) GIOKON 3500 series pressure cells were used (2 for each rehabilitated section) located approximately over the external "imprint" on the lane and separated between each other with a distance of 9.0 m (Figure 1). These cells were installed with the purpose of determining vertical compressive stresses produced in the rehabilitation overlay interface and the existing asphalt layer, as a response to loads imposed by traffic.

3. Results and Discussion

3.1 *Structure modeling and field validation*

(Table 4) and (Table 5) show the module of elasticity obtained in the back-calculation process for UHPFRC and MSC, respectively. The difference between laboratory results and those obtained in modeling is explained when considering the ideal conditions in which laboratory tests were executed, in comparison to the real on-site installation conditions determined with FWD.

The projection of a traffic of 43 million axis, equivalent to a 10-year period, was obtained from the project's original information. This number of axis corresponds to an exponential growth model, with a growth rate of 4.11%. Traction failure criterion in the lower MSC fiber and failure due to compression at the subgrade, were evaluated using Shell fatigue laws, according to (Equation 1) and (Equation 2).

Table 4. *Comparison of Modulus of elasticity at the laboratory vs UHPFRC back-calculation*

No.	Module at the laboratory (MPa)	Module per back-calculation (MPa)
1	45,728	39,000
2	41,409	36,000
3	41,692	
4	41,692	
5	37,755	
Average	41,655	37,000

Table 5. *Comparison of Modulus of elasticity at the laboratory vs MSC back-calculation*

No.	Module at the laboratory (MPa)	Module per back-calculation * (MPa)
1	5,860	3,160
2		2,880
Average	5,860	3,020

** Adjusted by temperature.*

1. *Permissible traction deformation in asphaltic layers*

Where

$$\varepsilon_{adm} = (0.856 * Vb + 1.08) * E^{-0.36} * (\frac{N}{K})^{-0.2} \qquad (1)$$

εadm: *Permissible traction deformation in asphaltic layers*
Vb: Asphalt percentage in the mix in volume (%)
E: Asphaltic mix dynamic modulus (N/m²)
N: Axis equivalent to 8,2 tons
K: Calage Coefficient

Revista Ingeniería de Construcción. RIC
Vol 37 Nº3 2022 www.ricuc.cl
DOI: 10.7764/RIC.00038.21

2. *Permissible compressive deformation in the subgrade*

$$\varepsilon_{adm} = 0.021 * N^{-0.25} \quad (2)$$

Where

εadm: *Permissible traction deformation in asphaltic layers*

N: Axis equivalent to 8.2 tons

(Table 6) and (Table 7) show modelling results of structures rehabilitated with MSC and UHPFRC, respectively.

Table 6. Modeling result of a structure rehabilitated with MSC-19
MG: Granular Material

Point	***Structure Thicknesses (cm)***				***Dynamic Module (MPa)***				***Equivalent Permissible Axis***	
									Failure Criterion MSC	***Criterion Rutting***
	MSC		MG	Total	MSC		MG	SR	*Shell CA*	*Shell*
1	21		50	71	3,160		350	160	*2.191E+08*	*1.272E+09*
2	21		50	71	2,880		210	150	*7.191E+07*	*7.452E+08*
	Average Values				3,020		280	155	*145,504,297*	*1,008,576,401*

MG: Granular Material

Table 7. Modeling result of a structure rehabilitated with UHPFRC

Point	***Structure Thicknesses (cm)***				***Dynamic Module (MPa)***				***Equivalent Permissible Axis***	
									Failure Criterion MSC	***Criterion Rutting***
	UHPFRC	MSC	MG	Total	UHPFRC	MSC	MG	SR	*Shell MSC*	*Shell*
1	4	17	50	71	39,000	2,500	250	150	*2.083E+08*	*2.003E+09*
2	4	17	50	71	36,000	3,000	300	156	*3.200E+08*	*2.744E+09*
	Average Values				37,500	2,750	275	153	*264,157,422*	*2.373.542.388*

MG: Granular Material

The criterion that rules the performance of the two resulting structures is fatigue failure of MSC. This result is aligned with research in development made by (Asphalt Institute, 1981) and with studies presented by (Orobio and Gi, 2015). Given the thicknesses and stiffness of the existing structure, stresses for supporting the subgrade are minimal.

It can be highlighted that a 40 mm replacement of UHPFRC represents an increase in the useful life of a structure, in terms of equivalent axis (ESALS in its English acronym) of 82%, considering traffic projections. This increase can be analyzed as 15 more years of service life; and is comparable to the case studies of Tayabi et ál., for Federal Highway Administration (FHWA), after analyzing kilometers of binded UTW overlays constructed in different territories of United States, the authors conclude that "UTW overlays that are properly designed and constructed can provide a useful life in at least 15 years and even possibly more than 20 years" (Tayabji et ál., 2009).

In order to conduct a validation of the model, data from pressure cells and the typology of vehicles associated to a response magnitude were taken. (Figure 2) shows the typical values of registered readings. The results of the field model were verified through a controlled load test (Figure 3), using a C3 type vehicle (simple steer axle and tandem 2-wheel rear axis) which circulated at three (3) different speeds, 20 km/h, 40 km/h and 60 km/h. Additionally, pressure values registered for this controlled reference load are displayed in (Figure 2).

DOI: 10.7764/RIC.00038.21

***Figure 2**. Maximum pressure values reported during the evaluation of test sections*

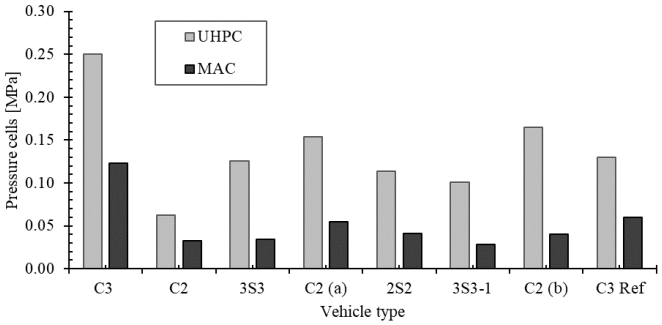

***Figure 3**. Reference load test*

	Front axle	Rear axle
	61.68	165.24
	61.98	164.95
Average	61.83	165.1
Half rear axle		**82.55**

According to modeling results, there were expected readings close to 0.4 MPa for UHPFRC and close to 0.074 MPa for MSC upon the passing of the reference controlled load (Table 8). However, the readings reported by cells displayed a maximum value of 0.2 MPa for UHPFRC and 0.06 MPa for MSC. Other studies report similar deviations in the comparison of theoretical vertical stress and those measured on the field. Particularly, it is worth to highlight studies carried out by Laboratorio Nacional de Materiales y Modelos Estructurales de la Universidad de Costa Rica (Lanamme UCR), which conclude that the results of modelling through finite elements are outside of the range of responses obtained in the field. The study shows that the value obtained in modeling (4.35 kPa) surpasses the maximum value recorded in field data (2.72 kPa) (Arias and Wang-Qiu, 2019)

***Table 8**. Vertical stress calculated through back-calculation for UHPFRC and MSC*

Material	***Modulus of Elasticity (MPa)***	***Sress ZZ (MPa)***	***Material***	***Modulus of Elasticity (MPa)***	***Sress ZZ (MPa)***
UHPFRC	39,000	0.4043	MSC	3,160	0.08070.0807
	36,000	0.4300		2,880	0.0673
	Average Values	0,4172			0.0740

From these results, it is inferred that in-service conditions, the performance of UHPFRC surpasses the one estimated in mathematical models and that the overlay thickness could be lower than 40 mm installed in this research. However, these results must be interpreted with caution, reason for which it is advised to deepen knowledge in instrumentation methodologies and carrying out modeling with alternative methods that consider the structure comprised by the UHPFRC layer and the existing asphaltic mix.

As a limiting factor, considering that the sensitiveness of cells in relation to the point of load application, it was not possible to verify the estress during the passing of controlled load right in the cell's axis. However, cell sensitiveness, to the distance of load

Revista Ingeniería de Construcción. RIC
Vol 37 Nº3 2022 www.ricuc.cl
DOI: 10.7764/RIC.00038.21

application, is coherent with the model's results, given that for the UHPFRC section, the result of vertical stress obtained at 0.16 m from the evaluation point (which would correspond to the pressure cell's central axis) is reduced from 0.430 MPa to 0.114 MPa.

3.2 Functional evaluation of the UHPFRC rehabilitated section

In order to evaluate the condition of the UHPFRC rehabilitated section through the PCI method, the section was divided in a grid with segments of 1.0 m x 1.15 m (Figure 4). The results of inspections showed a premature deterioration in panels identified as segments 5-1, 4-2, and 4-3. This deterioration began with the appearing of a transversal crack registered during the two first months of opening the section for service. Failure evolved throughout the following months affecting segments 4-1, 4-2, 4-3, 5-1, 5-2 and 5-3. (Figure 4) shows the distribution and classification of identified damage areas. Pathology occurred due to a process that was not properly carried out in the casting of concrete, which emerged in short time. In addition, it was evidenced that after the end of the research, that the section which presented premature damages was installed with a thickness inferior to 30 mm. Studies related to the construction of UTW overlayers (Haber et al, 2017); (Khazanovich and Tompkins, 2017); (Harrington and Fick, 2014); (Wiegand et al, 2010); (Russell and Graybeal, 2013) show the use of truss type vibratory equipment or vibratory rulers (magic screed) and industrial paving MSChines for working on layers in bridge panels. However, in this research, due to the thickness (40 mm) of the overlay and the type of material with self-leveling characteristics, it was decided not to include any type of vibration.

From the calculated data, it was observed that over the evaluated UHPFRC layer, there were no damages caused by construction deficiencies, these presented a PCI rating above 90. In other words, it classifies within the "Excellent" category.

***Figure 4**. Identification of failures in the UHPFRC section divided by sections for follow up.*

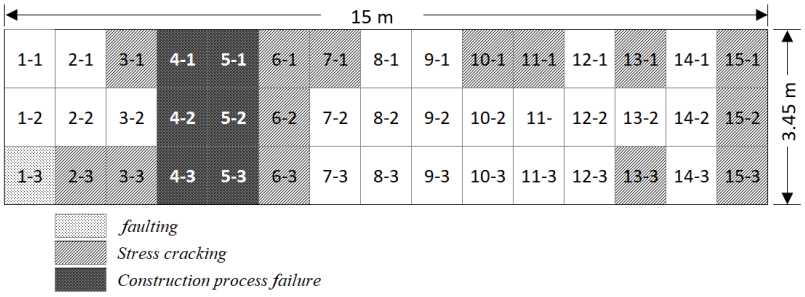

(Figure 5) shows a comparison of the PCI rating excluding the six segments that were affected by the constructive process (with no construction induced damages) and the rating that includes the segment with failures (with construction induced damages).

***Figure 5**. PCI values for the UHPFRC section*

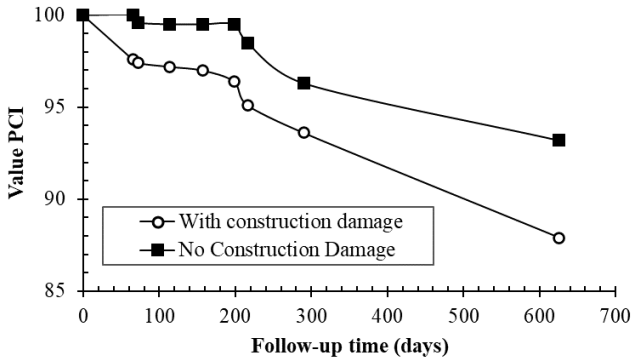

Some inconveniencies with the placing and casting operation of UHPFRC caused interruptions in the casting of concrete; these lasted for approximately 15 minutes, while the zone corresponding to segments 5 was being installed (section which presented premature deterioration). The performance of fresh concrete is sensitive to time and if UHPFRC is allowed to rest during a prolonged time period (only 3 to 5 minutes), the internal concrete structure begins to accumulate and may lose capacity to self-consolidate and flow (Ribeiro Furtado de Mendonca et ál., 2020). Because of this, this delay in casting caused a "false curing" effect in the lower UHPFRC fiber, which hindered the correct binding between UHPFRC and the underlying asphaltic mix. In turn, this generated a "cantilever" layer effect.

DOI: 10.7764/RIC.00038.21

Demolition of the test section evidenced that in grid squares 4 and 6 the overlay thickness was below 30 mm, (less than the projected 40 mm). Errors in the construction process generated support failures and insufficient adhesion to the underlying layer, in addition to thicknesses under the established value. This translated into a premature deterioration that spread through segments 4.1, 4.2, 4.3, 5.1, 5.2, and 5.3. (Figure 6) shows the evolution of deterioration.

Figure 6. *Evolution process of premature deterioration vs section with no damages.*

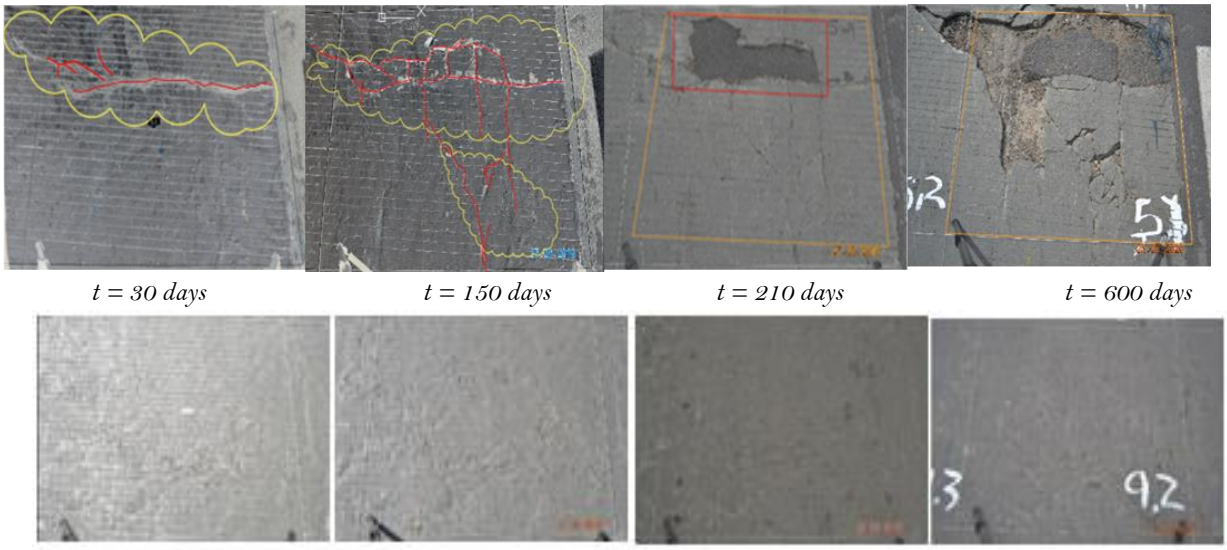

According to (Khazanovich and Tompkins, 2017) UTW overlays are very sensitive to installation operations, as well as the preparation of the support surface and seam cutting; because of this, these overlays can display early failures (Khazanovich and Tompkins, 2017).

According to the analysis by segments (Figure 7) it was identified that 51% of the slab did not present damages. Close to 7% of the segments registered early cracking due to curing, which did not show any progression during 9 months of follow up. 15% of segments presented longitudinal cracks in areas close to the slab seams. These appeared between month 9 and 18 (last visual inspection of the section); these cracks are generated due to a phenomenon associated to the interface's tensile stresses, and, are mainly induced by loads that are proximal to edges and corners (Mu and Vandenbossche, 2010). Considering that the performance of in-service overlays indicates mode of real failure depends more on the size of the slab than on its thickness (Li and Vandenbossche, 2013), it is advised to study this effect in future developments related to the large scale use of UHPFRC.

In this study, it was not possible to establish if the UHPFRC section of 15 m x 3.45 m would require transversal seams or panels of smaller size, given that constructive failure generated a transversal breaking of the slab. However, it is worth to highlight that between grid squares 6 to 15 there was no observed need for transversal seams with a length of less than 10 given that the distribution of seams implies a work load, and therefore, an increase in construction costs (Suh et ál., 2008). It is advised to conduct studies geared towards determining the ideal geometry of UHPFRC overlays with thicknesses below or equal to 50 mm. Additionally, it is recommended to study the incidence of the warpage phenomenon in large surfaces constructed with UHPFRC.

Resistance of a pavement to friction depends on the microtexture of aggregates and the MSCrotexture of pavement's surface (Lu and Steven, 2006). UHPFRC is a material that lacks coarse aggregates; at first instance, this could entail difficulties for reaching the minimum friction values recommended in the Guide for Pavement Friction which is 0,5 – 0,55 (National Academies of Sciences, Engineering, and Medicine, 2009). However, readings obtained with the British pendulum TRRL were satisfactory, as shown in (Figure 8). The trend is congruent with results of other research efforts, which support that, for the case of new pavements it is expected to have an increase in their friction coefficient in as the superficial binder is removed due to the effect of vehicle transit, until it reaches a point in which superficial friction only depends on the aggregate's properties. Posteriorly a stage of aggregate polishing begins, when the superficial friction drops until it stabilizes (Herra and Gómez, 2019). In the absence of coarse aggregates, this behavior can be associated to the surface formation of a layer known as "elephant skin", comprised by a dense and dark upper layer with a high resistance to abrasion; posteriorly, a layer characterized by its shine and low abrasion resistance is observed (Wetzel and Glotzbach, 2013).

Revista Ingeniería de Construcción. RIC
Vol 37 Nº3 2022 www.ricuc.cl
DOI: 10.7764/RIC.00038.21

***Figure 7**. Friction coefficient resistance in the test section (UHPFRC and MSC-19)*

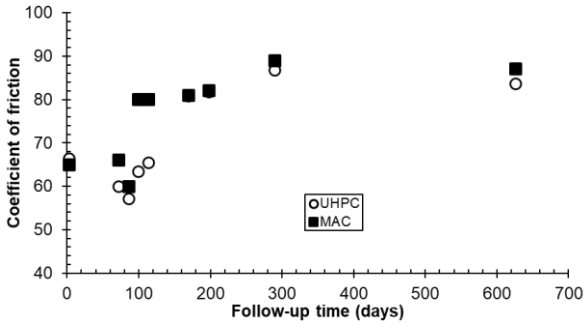

The section constructed with UHPFRC was not microtexturized, considering the viscoelastic behavior of this material. According to (Wetzel and Glotzbach (2013) the "elephant skin" phenomenon limits the possibility of softening concrete's surface.

Another relevant aspect in the functional evaluation of a pavement is the International Roughness Index, which is usually measured in m/km and is the most used index for the development of deterioration models in pavements (Piryonesi and El-Diraby, 2021)

(Figure 8) shows profile details of both test sections; the IRI results were of 2.73 m/km for MSC-19 and 3.05 m/km for UHPFRC.

***Figure 8**. Profiles obtained for the IRI calculation in test sections with MSC and UHPRFC.*

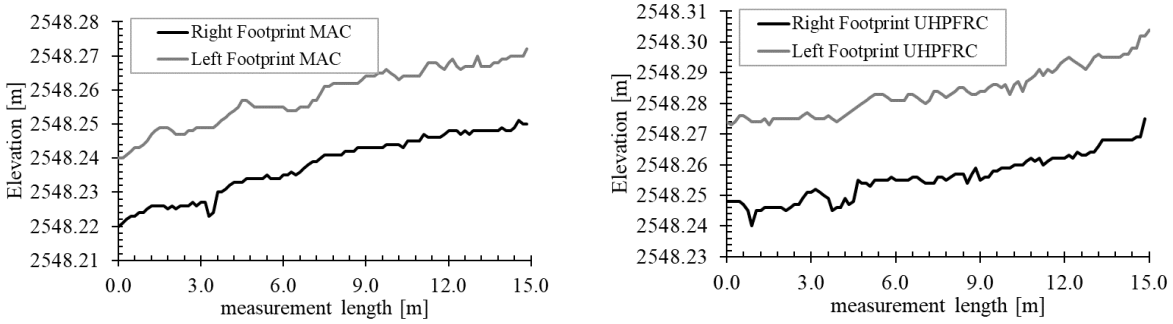

For the UHPFRC section, the IRI value is out of the average acceptance range, as can be observed in (Table 9).

***Table 9**. Limit IRI values for new or reconstructed roads*

Country	*Specification*	*Limit IRI vale for new or reconstructed roads m/km*
Australia	*AC/PCC Highways and main roadways (100km/h)*	*1.9*
El Salvador- –	*PCC- Inter urban roadways*	*2.5*
Philippines-	*AC/PCC Primary national roadways*	*3.0*
Russia -	*AC/PCC First class roads and roadways*	*2.2*
Belarus	*AC/PCC – reconstruction of first-class roadways*	*2*
Chile	*AC/ PCC Surface treatment*	*2.4 (50%), 2.9 (85%), 3.4 (99%*
Colombia	*PCC*	*3*
Italy	*PCC first-class*	*2.5*
Kazajstan	*AC / PCC – highways and first-class roads*	*2.4*

DOI: 10.7764/RIC.00038.21

Lithuania	*AC/PCC – main roadways*	*1.5*
Slovakia	*AC/PCC – - primary and secondary roadways*	*1.9*
Hungary	*Main roadways*	*1.2*

AC – Asphaltic concrete pavement.
PCC – Hydraulic concrete pavement
Adapted based on data from Múčka (2017).

The IRI value obtained for UHPFRC is attributed to construction deficiencies generated by the equipment used for extension, as well as the lacking of a guiding formwork that guarantees a correct longitudinal profile.

4. Conclusions

A 40 mm replacement of asphaltic mix with UHPFRC represents an increase of life span in the pavement structure in terms of equivalent axis of 8.2 tons of 80%, in its lifecycle, this could represent an approximate increase of 15 years.

Premature deterioration of the UHPFRC rehabilitated section did not allow to establish the need of inducing cracking due to curing retraction (seams) at a distance smaller than 15 meters of length in the section. Findings agree with studies from other authors, who show that seams close to the wheel axis generate stresses, which in tur, produce longitudinal cracks.

In a length of 10 m, the UHPFRC overlay did not evidence the need of transversal seams; this could be due to a substantial improvement in the Whitetopping technique used, along with the reduction of construction costs and maintenance associated to seams.

Like conventional concretes, UHPFRC is extremely susceptible to the installation process; constructive deficiencies affected the following:

- *International Roughness Index (IRI), which presents a value of 3.05 m/km.*
- *Sectors with smoothness values above 5mm.*
- *Average thicknesses inferior to those designed*

Despite displaying premature failure attributed to a deficient installation process, the UHPFRC test section did not present typical damages that can be attributed to UWT: breaking of corners, chipping of seams.

According to (Graybeal y El-Helou, 2019) the following long-term challenges are acknowledged: the availability of materials for the UHPFRC mix, availability of appropriate installing equipment and proper training of the labor force.

5. Acknowledgements

The authors of this work acknowledge and thank the support given by Cementos Argos S.A, Minciencias (Project No. 63881. Agreement 125-2019), concesiones CCFC SAS, and the Civil Engineering Department of the Pontificia Universidad Javeriana.

6. References

Ahmed, F.; Thompson, J.; Kim, D.; Carroll, E.; Huynh, N. (2020). Cost-effectiveness of performing field investigation for pavement rehabilitation design of non-interstate routes. International Journal of Transportation Science and Technology, 10(3), 299-301. https://doi.org/10.1016/j.ijtst.2020.06.001

Arias-Barrantes, E.; Wang-Qiu, S. Q. (2019). Instrumentación de estructuras de pavimento. Boletín Técnico PITRA - LanammeUCR, 10(6). https://www.lanamme.ucr.ac.cr/repositorio/handle/506251125OO/1591

Asphalt Institute. (1981). Thickness design: asphalt pavement structures for highways and streets. Asphalt Institute.

ASTM International. (2021). ASTM E1926-08. Standard practice for computing international roughness index of roads from longitudinal profile measurements. ASTM International. https://doi.org/10.1520/E1926-08R21

Graybeal, B.; El-Helou, R. G. (2019, 2-5 de junio). Development of an AASHTO Guide Specification for Ultra-High Performance Concrete [Presentación de escrito]. International Interactive Symposium on Ultra-High Performance Concrete, Albany, New York, Estados Unidos. https://doi.org/10.21838/uhpc.9708

Graybeal, B. A. (2006). Material Property Characterization of Ultra-High Performance Concrete (Publicaition No. FHWA-HRT-06-103). U.S. Department of Transportation, Federal Highway Administration. https://rosap.ntl.bts.gov/view/dot/38714

Green, B.; Moser, R.; Scott, D.; Long, W. (2014). Ultra-High Performance Concrete History and Usage by the Corps of Engineers. Advances in Civil Engineering Materials, 4(2), 132-143. https://www.astm.org/acem20140031.html

DOI: 10.7764/RIC.00038.21

Haber, Z. B.; Munoz, J. L.; Graybeal, B. A. (2017). Field Testing of an Ultra-High Performance Concrete Overlay [Technical report FHWA-HRT-17-096]. Federal Highway Administration. https://rosap.ntl.bts.gov/view/dot/37821

Harrington, D. S. (2014). Guide to Concrete Overlays: Sustainable Solutions for Resurfacing and Rehabilitating Existing Pavements (3rd ed.). American Concrete Pavement Association. https://rosap.ntl.bts.gov/view/dot/17114/

Herra, L.; Gómez, H. (2019). Evolución de la fricción superficial en pavimentos asfálticos. Boletín Técnico PITRA - LanammeUCR, 10(4). https://www.lanamme.ucr.ac.cr/repositorio/handle/50625112500/1434

Hungria, R.; Arce, G.; Hassan, M.; Anderson, M.; Mahdi, M.; Rupnow, T.; Bogus, S. M. (2020). Evaluation of novel jointless engineered cementitious composite ultrathin whitetopping (ECC-UTW) overlay. Construction and Building Materials, 265, 120659. https://doi.org/10.1016/j.conbuildmat.2020.120659

Khazanovich, L.; Tompkins, D. (2017). Thin concrete overlays. TechBrief, FHWA-HIF-17-012. https://www.fhwa.dot.gov/pavement/pubs/hif17012.pdf

Koutný, O.; Snoeck, D.; Van Der Vurst, F.; De Belie, N. (2018). Rheological behaviour of ultra-high performance cementitious composites containing high amounts of silica fume. Cement and Concrete Composites, 88, 29-40. https://doi.org/10.1016/j.cemconcomp.2018.01.009

Larsen, I. L.; Thorstensen, R. T. (2020). The influence of steel fibres on compressive and tensile strength of ultra high performance concrete: A review. Construction and Building Materials, 256, 119459. https://doi.org/10.1016/j.conbuildmat.2020.119459

Li, Z.; Vandenbossche, J. M. (2013). Redefining the Failure Mode for Thin and Ultrathin Whitetopping with 1.8- × 1.8-m Joint Spacing. Transportation Research Record, 2368(1), 133-144. https://doi.org/10.3141/2368-13

Lu, Q.; Steven, B. (2006). Friction Testing of Pavement Preservation Treatments: Literature Review. UC Davis: University of California Pavement Research Center. https://escholarship.org/uc/item/3jn462tc

Marcomini Pinatt, J.; Chicati, M. L.; Ildefonso, J. S.; D'arce Filetti, C. R. G. (2020). Evaluation of pavement condition index by different methods: Case study of Maringá, Brazil. Transportation Research Interdisciplinary Perspectives, 4, 100100. https://doi.org/10.1016/j.trip.2020.100100

Mateos, A.; Harvey, J.; Paniagua Fernandez, F.; Paniagua, J.; Wu, R. (2019). Accelerated Testing of Full-Scale Thin Bonded Concrete Overlay of Asphalt. Transportation Research Record: Journal of the Transportation Research Board, 2673(2), 404-414. https://doi.org/10.1177/0361198119825645

Mu, F.; Vandenbossche, J. (2010, 10-11 de octubre). Temperature Effects on Overlay Bond Characteristics andthe Overlay Response to Dynamic Loads for Bonded PCC Overlays Placed on Asphalt Pavements [Presentación de escrito]. 7th International DUT-Workshop on Design and Performance of Sustainable and Durable Concrete Pavements, Carmona, España. https://www.researchgate.net/publication/275023379_Temperature_Effects_on_Overlay_Bond_Characteristics_andthe_Overlay_Response_to_Dynamic_Loads_for_Bonded_PCC_Overlays_Placed_on_Asphalt_Pavements

Múčka, P. (2017) International Roughness Index specifications around the world. Road Materials and Pavement Design, 18(4), 929-965, https://doi.org/10.1080/14680629.2016.1197144

National Academies of Sciences, Engineering, and Medicine. (2009). Guide for Pavement Friction. The National Academies Press. https://doi.org/10.17226/23038

Orobio, A.; Gil, J. (2015). Construction cost analysis related to the mechanistic design of pavements with different fatigue models. Revista Ingeniería de Construcción, 30(3), 177-188. https://www.ricuc.cl/index.php/ric/article/view/526

Piryonesi, S. M.; El-Diraby, T. E. (2021). Examining the relationship between two road performance indicators: Pavement condition index and international roughness index. Transportation Geotechnics, 26, 100441. https://doi.org/10.1016/j.trgeo.2020.100441

Quist Batista, C. M.; Rowland, L.; Nielsen, E. P. (2019, 2-5 de junio). The Next Generation of UHPC [Presentación de escrito]. International Interactive Symposium on Ultra-High Performance Concrete, Albany, New York, Estados Unidos. https://doi.org/10.21838/uhpc.9698

Ribeiro Furtado de Mendonca, F.; El-Khier, M. A.; Morcous, G.; Hu, J. (2020). Feasibility Study of Development of Ultra-High Performance Concrete (UHPC) for Highway Bridge Applications in Nebraska. Nebraska Department of Transportation Research Reports, 242. https://digitalcommons.unl.edu/ndor/242

Russell, H. G.; Graybeal, B. A. (2017). Ultra-High Performance Concrete: A State-of-the-Art Report for the Bridge Community [Technical report FHWA-HRT-13-060]. Federal Highway Administration. https://rosap.ntl.bts.gov/view/dot/26387

Shi, C.; Wu, Z.; Xiao, J.; Wang, D.; Huang, Z.; Fang, Z. (2015). A review on ultra high performance concrete: Part I. Raw materials and mixture design. Construction and Building Materials, 101, Part 1, 741-751. https://doi.org/10.1016/j.conbuildmat.2015.10.088

Suh, C.; Kim, D.; Won, M. C. (2008). Development of the Thickness Design for Concrete Pavement Overlays over Existing Asphalt Pavement Structures (FHWA/TX-09/0-5482-2). Article FHWA/TX-09/0-5482-2. Center for Transportation Research, The University of Texas at Austin. https://trid.trb.org/view/890429

DOI: 10.7764/RIC.00038.21

Suksawanga, N.; Alsabbaghb, A.; Shabanc, A.; Wtaife, S. (2020). Using post-cracking strength to determine flexural capacity of ultra-thin whitetopping (UTW) pavements. Construction and Building Materials, 240, 117831. https://doi.org/10.1016/j.conbuildmat.2019.117831

Tayabji, S.; Gisi, A.; Blomberg, J.; DeGraaf, D. (2009, 21-24 de abril). New applications for thin concrete overlays: Three case studies [Presentación de escrito]. National conference on preservation, repair, and rehabilitation of concrete pavements, St. Louis Missouri, Estados Unidos. https://rosap.ntl.bts.gov/view/dot/25961

Wetzel, A.; Glotzbach, C. (2013, 10-14 de junio). Microstructural Characterisation of Elephant Skin on Ultra-High Performance Concrete [Presentación de escrito]. 14th Euroseminar on Microscopy Applied to Building Materials, Helsingor, Dinamarca. https://doi.org/10.13140/2.1.4970.1123

Wiegand, P. D.; Cable, J. K.; Cackler, T.; Harrington D. (2010). Improving Concrete Overlay Construction. Iowa Highway Research Board; Federal Highway Administration. https://rosap.ntl.bts.gov/view/dot/18060/

Xue, J.; Briseghella, B.; Huang, F.; Nuti, C.; Tabatabai, H.; Chen, B. (2020). Review of ultra-high performance concrete and its application in bridge engineering. Construction and Building Materials, 260, 119844. https://doi.org/10.1016/j.conbuildmat.2020.119844

Zhou, M.; Lu, W.; Song, J.; Lee, G. C. (2018). Application of Ultra-High Performance Concrete in bridge engineering. Construction and Building Materials, 186, 1256-1267. https://doi.org/10.1016/j.conbuildmat.2018.08.036